Effective Band Structure of Random Alloys

Voicu Popescu and Alex Zunger*

National Renewable Energy Laboratory, Golden, Colorado 80401, USA

(Received 16 April 2010; published 11 June 2010)

Random substitutional A_xB_{1-x} alloys lack formal translational symmetry and thus cannot be described by the language of band-structure dispersion $E(\vec{k})$. Yet, many alloy experiments are interpreted phenomenologically precisely by constructs derived from wave vector $\vec{k}$, e.g., effective masses or van Hove singularities. Here we use large supercells with randomly distributed A and B atoms, whereby many different local environments are allowed to coexist, and transform the eigenstates into an effective band structure (EBS) in the primitive cell using a spectral decomposition. The resulting EBS reveals the extent to which band characteristics are preserved or lost at different compositions, band indices, and $\vec{k}$ points, showing in (In,Ga)N the rapid disintegration of the valence band Bloch character and in Ga(N,P) the appearance of a pinned impurity band.

DOI: 10.1103/PhysRevLett.104.236403 PACS numbers: 71.23.An, 71.55.Eq

Introduction: Do random alloys have a band structure? Design of substitutional A_xB_{1-x} alloys is one of the leading approaches in metallurgy [1], ceramics and semiconductor [2,3] technologies to create functionalities that are intermediate between those offered by the end point constituent solids A and B. Perhaps the most important characteristic of such random substitutional alloys is the absence of translational long range order and its replacement by a distribution of many local environments, giving rise to what will be called a polymorphous configuration. Indeed, in the alloy, an A atom may be coordinated locally by varying numbers of A and B neighbors; such local motifs are distributed (either randomly or in a correlated fashion) throughout the alloy sample. Manifestations of such periodicity-removing fluctuations in substitutionally random alloys include the existence of a distribution of different types of bonds [4], carrier [5] and exciton [6,7] localization, or the formation of impurity states within the otherwise forbidden band gap [5]. In metal alloys, the charge on a particular A atom will depend critically if it is coordinated locally mostly by like A atoms or by unlike B atoms [8]. Considering the existence of polymorphous configurations [9–11] with attendant loss of periodicity in random alloys, one will be inclined to accept that such alloys do not have energy bands, thus rejecting the wave vector and the band structure as viable concepts. This view represents a departure from the historic tradition of replacing for the polymorphous picture by a repetition of a single or two motifs, as in the virtual crystal approximation [3] the band anticrossing model [12], or the coherent potential approximation [3,13]. Such a restoration of the symmetry of the constituent solids A and B into the alloy framework not only leads to a major computational simplification, but also reestablishes the language of band theory $E(\vec{k})$ as appropriate to disordered alloys. This approach is paralleled by similar tradition in experimental interpretation of random alloys phenomena in terms of concepts akin to wave vectors $\vec{k}$ and dispersion relations $E(\vec{k})$. This includes the association of effective mass $m^* \propto [\partial^2 E/\partial k_\alpha \partial k_\beta]^{-1}$ with alloys [12,14], or van Hove singularities in alloy reflectivity spectra [15], effective band dispersion deduced from either magnetotunneling spectroscopy [16] or from alloy angular-resolved photoemission spectroscopy [17]. In all of these experiments one measures an alloy property (lacking in principle wave vector representation) and equates it with a translationally invariant *model*, backing out from this imposed equality some effective band structure $E(\vec{k})$ and its ensuing derivative quantities. What is not conveyed by such phenomenological approaches [12–17] is the *extent* to which this bandlike picture is preserved as one moves from a band edge to other locations in the Brillouin zone, or as the alloy composition x in A_xB_{1-x} is varied, or as we move from band-edge states to higher energy bands.

We use here an approach that generates what will be called an ''effective band structure'' (EBS) for disordered alloys in the primitive Brillouin zone of the parent compounds. But unlike models that discard fluctuations at the outset [3,12,13], the present approach is based on a fully polymorphous supercell (SC) description of the alloy. The substitutionally disordered alloy is first described using large SCs, containing possibly thousands of atoms with randomly (or correlated) distributed site occupations, allowing for polymorphous configurations. Diagonalization of the SC Hamiltonian provides the alloy eigenstates $\{\varepsilon_i, |\Psi_i\rangle\}$. Second, one is calculating the amount of Bloch character $\vec{k}$ preserved in these alloy states. The choice of the Brillouin zone in which $\vec{k}$ is confined can be completely independent of the choice and symmetry of the SC. Thus, following the requirement that the correct ensemble average of the charge density in a substitutional alloy has the periodicity of the underlying lattice, we *end up* with the symmetry of the constituents but we start with a lower symmetry of the SC. Unfolding the SC results into the

chosen Brillouin zone leads to a dispersion relationship that conveys the effects of existence of a multitude of local environments through broadening and dispersion of the effective $E(\vec{k})$ relation of the EBS. This is important because it allows us to assess the relevance of the phenomenological interpretations described above for any substitutional alloy. The EBS further enables us to calculate an "effective" effective mass m^{**}, a term that shall be associated with the gradient of alloy EBS, in a similar way as the effective mass m^* is associated with the gradient of the band structure $E(\vec{k})$ of crystalline periodic solids.

Method.—Our method is based on spectral decomposition used previously [9,18,19]. To describe a random substitutionally alloy we use large supercells (SC) whose lattice vectors are in relation to an underlying primitive cell (PC), as illustrated by the two-dimensional example in Fig. 1. We denote by $\vec{k}$ ($\vec{K}$) the wave vectors corresponding to the PC (SC) reciprocal space, with lattice vectors $\vec{g}$ ($\vec{G}$). The Brillouin zone vectors of the two spaces obey the folding relation $\vec{K} = \vec{k} + \vec{G}$.

We calculate thousands of alloy SC eigenstates $\{\varepsilon_i, |\Psi_{i\vec{K}}\rangle\}$ and derive a spectral function (SF) of continuous variable E:

$$A(\vec{k}, E) = \sum_i |\langle \Psi_{i\vec{K}} \mid \vec{k}\rangle|^2 \delta(\varepsilon_i - E), \qquad (1)$$

where $|\vec{k}\rangle$ is a Bloch state of wave vector $\vec{k}$ of the underlying PC and the spectral weight $|\langle \Psi_{i\vec{K}} \mid \vec{k}\rangle|^2$ quantifies the amount of Bloch character preserved in the SC eigenvector $|\Psi_{i\vec{K}}\rangle$ [9,18]. Obviously, for a *periodic* system, the spectral weight is either 1 or 0, depending on whether ε_i corresponds to an eigenvalue at $\vec{k}$ or not, whereas for SCs describing *random alloys*, it will take on any value between 0 and 1. Applying Eq. (1) for a series of primitive wave vectors $\vec{k}_j = \vec{K} + \vec{G}_j$, we obtain a collection $\{A(\vec{k}_j, E)\}$ of SFs. A useful quantity is the cumulative sum [19] $S(\vec{k}_j, \varepsilon_n) = \int^{\varepsilon_n} A(\vec{k}_j, E)dE$ which is characterized by steps of value 1 whenever an "alloy band" is crossed [19], and

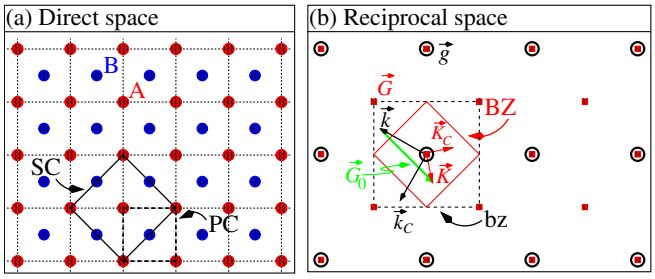

FIG. 1 (color online). Two-dimensional illustration of the relation between a supercell (SC) and a primitive cell (PC) direct (a) and reciprocal spaces (b) of an ordered *AB* lattice. In panel (b), squares (circles) denote SC (PC) reciprocal lattice vectors. $\vec{K} = \vec{k} + \vec{G}_0$ illustrates a folding relation PC $\mapsto$ SC. Brillouin zone vectors $\vec{k}$ and $\vec{k}_C$ ($\vec{K}$ and $\vec{K}_C$) are symmetry related if C is a symmetry operation of the crystal.

thus allows one to estimate the alloy bands positions and widths. In the following, a $\vec{k}$-dependent band width is the energy range in which $A(\vec{k}, E) \geq 10^{-3}$ around a band center. We obtain the EBS by collecting all of the SFs and the band widths in single E versus $\vec{k}$ plots, as those shown in Figs. 2(a)–2(e).

Two averaging steps are important when determining the random alloy EBS: first, for a given random configuration, we enforce the *macroscopic* symmetry of the alloy, by averaging $A(\vec{k}, E)$ over all symmetry-related $\vec{k}$ vectors. If the system were periodic, with C one of its symmetry operations, the PC (SC) wave vectors $\vec{k}$ and $\vec{k}_C = C\vec{k}$ ($\vec{K}$ and $\vec{K}_C = C\vec{k}$) would be equivalent, as shown in Fig. 1(b). For a *random alloy*, however, C is no longer a symmetry operation of the SC. We therefore explicitly calculate SC eigenstates for all the corresponding $\vec{K}_C = \vec{k}_C + \vec{G}$ vectors. Second, the procedure of collecting averaged SFs is repeated, at a given alloy composition, for several (in the following eight) random realizations. The SFs for alloys are thus broadened and structured, exhibiting a finite, $\vec{k}$-dependent band width, a direct consequence of the polymorphic nature of the adopted description. Once the EBS is available, we can calculate an effective band $E^*_m(\vec{k})$, numerically evaluate its curvature and thus to determine the effective effective mass m^{**} for electrons and holes.

Weakly perturbed alloys preserve the band structure.—Figure 2 shows the EBS for the weakly perturbed (In,Ga)N alloy in the zinc-blende structure. This system is characterized by a lattice mismatch of 7% and a small valence band offset of 0.26 eV [20]. The calculations have been performed using 512-atom supercells, allowing for valence force field full relaxation using the empirical pseudopotential of Ref. [21] in a plane-wave representation [9], neglecting the spin-orbit coupling.

Figures 2(a) and 2(e) show the band structure of GaN and InN binaries and their corresponding SFs. As expected for periodic systems, the SFs [red (gray) horizontal lines] appear as sharp, deltalike peaks at the points where $E(\vec{k})$ intersect a $\vec{k}$-point. For the $In_xGa_{1-x}N$ random alloy [panels (b) to (d)] effective alloy bands can be recognized for all compositions, appearing as broad peaks in the SFs and evidenced by the corresponding $\vec{k}$-dependent band widths [light blue (gray) shaded areas]. We see that the alloy preserves sharp, bandlike, SF peaks only at Γ and X points of the fcc Brillouin zone, and that the In-rich alloys are more Bloch-like than the Ga-rich alloys. A rapid loss of Bloch character occurs for intermediate $\vec{k}$ vectors at all compositions, consistent with the fact that sharp reflectivity features are seen only at Γ. This loss is more pronounced in the first conduction band (CB1), which broadens to 1 eV in the intermediate $\vec{k}$ range. This broadening originates from the convexity of CB1 resulting in eigenstates of different wave vectors having close eigenvalues and thus the folded states of the SC in a small energy

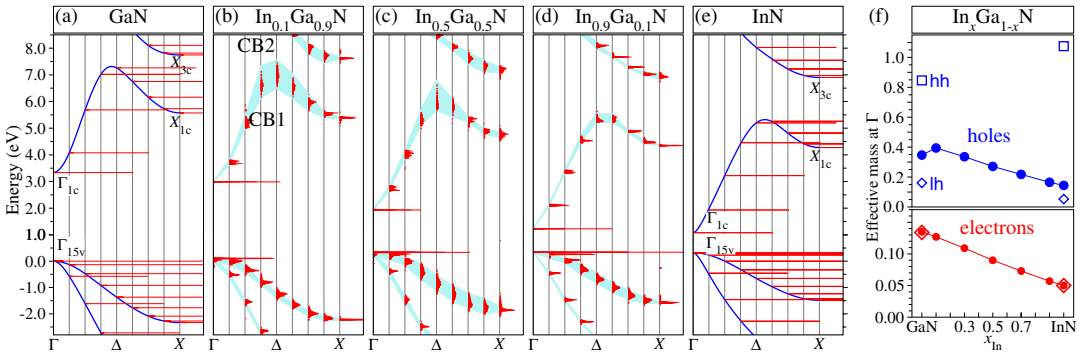

FIG. 2 (color online). EBS for (a) pure GaN, (e) pure InN, and for the $In_xGa_{1-x}N$ alloy (b)–(d). The different $\vec{k}$ vectors in the primitive cell are represented by thin vertical lines. Red (gray) lines represent the SFs $A(\vec{k}, E)$ at each such $\vec{k}$ point. For the random alloys, the SFs exhibit a finite, $\vec{k}$ dependent band width [light blue (gray) shaded areas]. (f): Effective effective mass m^{**} of electrons and holes in $In_xGa_{1-x}N$ at the Γ point (filled symbols). Open symbols refer to effective masses m^* for individual bands in the pure binaries.

range consist of an overlap of many different $\vec{k}$ states. In contrast to CB1, the valence bands and the second conduction band (CB2), have narrower $\vec{k}$-dependent widths for all $\vec{k}$'s, throughout the whole composition range. Our unfolding procedure allows one to observe the way various physical factors in the polymorphous representation translate into band-dispersion and broadening in the primitive cell description. For example, repeating the calculations for the $In_{0.5}Ga_{0.5}N$ alloy of Fig. 2(c) but using unrelaxed, ideal fcc positions in the original SC, revealed that relaxation alone reduces the broadening of the upper valence band by a factor of 3 relative to the unrelaxed case (not shown), and creates a rather sharp SF at the Γ point.

Since the (In,Ga)N alloy exhibits a well-defined EBS, one can calculate EBS-derived effective quantities. We show in Fig. 2(f) the composition dependence of the m^{**} for electrons and holes at the Γ point. For both type of carriers m^{**} has a monotonic, linear dependence on x_{In}. Because in the case of the valence band our procedure implies an average over three unresolved bands, we obtain that the hole m^{**} of pure binaries lies between the actual m^* calculated directly from the band structure [open symbols in Fig. 2(f)].

The strongly perturbed P-dilute GaN:P system reveals impurity band development.—The mixed-anion zinc-blende system Ga(N,P) typifies a strongly perturbed alloy [22,23], having a large valence band offset of 1.71 eV and lattice misfit (20%) [20]. Figure 3(a) shows that vanishingly small amounts of P in GaN lead to a strongly localized (t_2-like) level in the gap [24] evolving with increasing composition into an impurity band (IB).

The $\vec{k}$-resolved spectral functions of the IB ($\vec{k}$-resolved densities of states), show the following characteristics: (i) the maximum in each SF appears at the energy center of the IB, with its center of gravity being pinned in energy and varying very little with P composition; (ii) above and below the center of the IB one observes discrete levels, as the ones labeled E_1 and E_2 in Fig. 3(a); (iii) the Γ-SF is the dominant component, followed by a fast decay for the wave vectors near the zone edge. All these features are typical signatures of the disordered-driven, Anderson localization model [25]. The discrete levels above and below the center of gravity of the IB are due to localized states caused by various P-P pairs, as shown by the wave function plots in Fig. 4. We identify here the first-neighbor PP_1 and the fourth-neighbor PP_4 pairs, which are deeper for smaller P-P separations.

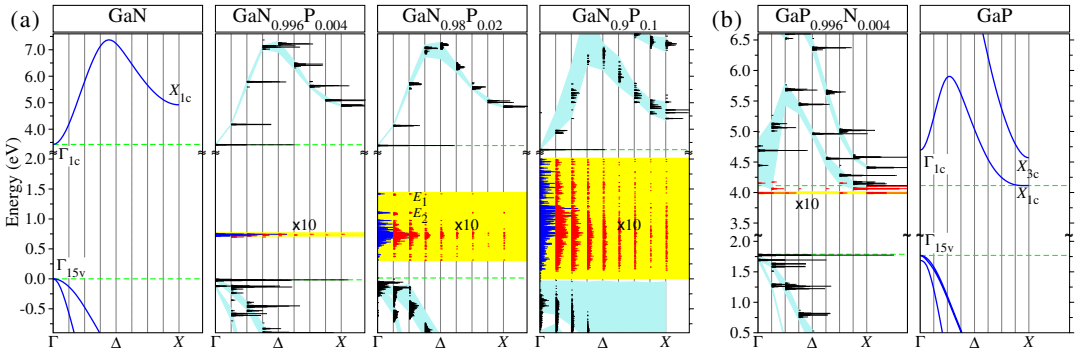

FIG. 3 (color online). Same as Fig. 2 but for (a) P-dilute GaN and (b) N-dilute GaP. E_1 and E_2 label two localized states corresponding to P-P pairs. Note the two different energy scales in (a) and (b).

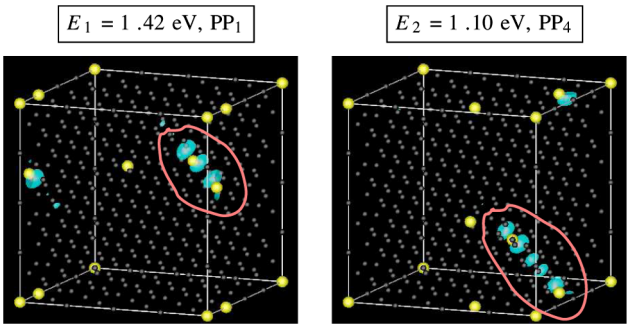

FIG. 4 (color online). Isosurfaces [cyan (gray)] of the two localized wave functions labeled E_1 and E_2 in Fig. 3(a) for $GaN_{0.98}P_{0.02}$, corresponding to PP_1 (E_1) and PP_4 (E_2) pairs. P atoms are depicted in yellow (light gray), all the other atoms in the SC are dark grey.

The increase of P content x_P leads to a rapid widening of the IB, which extends over $\simeq 1$ eV already at $x_P = 0.02$. Simultaneously, this increase also leads to a disintegration of the valence band. One can recognize its band structure at small values of x_P, but this structure rapidly vanishes for $x_P \geq 0.02$. Using larger, 4096-atom SCs, we have checked that this is not a small-cell size effect. The valence band maximum is practically pinned up to the valence-impurity band merging point (around $x_P = 0.1$), pinning caused by the localized states of the P-P pairs.

The N-dilute GaP:N system reveals hybridization between localized and extended states.—Below a critical nitrogen composition x_N (the ''amalgamation point'') one finds strongly localized, sharp N-cluster states with a broader continuum of perturbed host states above it [22], as shown in Fig. 3(b). In this x_N regime, the cluster states are predicted to stay pinned in energy, as observed experimentally by Fluegel *et al.* [26] in low temperature photoluminescence for $x_N < 0.1\%$ samples [27]. Once the amalgamation point is exceeded, there is a coexistence of cluster states with the perturbed host states. Beyond this x_N, a complete alloy behavior is seen, with levels shifting [27] with increasing x_N.

Features like (i)–(iii) described above for GaN:P are not present in the GaP:N system shown in Fig. 3(b). Indeed, we see that the N a_1 level has comparable projections at both Γ and X points of the fcc Brillouin zone. Our comparative study of GaN:P and GaP:N in the diluted limit shows clear qualitative differences, differences which are assigned to the different nature in the evolution of the two states: whereas the P-derived t_2 states evolve in a true IB in GaN:P, this is not the case for the N-derived a_1 states in GaP:N.

Conclusions.—We have shown that, while keeping the more appropriate polymorphous picture in describing the physical properties of disordered alloy via supercells, one can still obtain an effective band structure (EBS) in the underlying primitive cell. We applied this tool to (In,Ga)N and Ga(P,N) contrasting the preservation of the band character at high symmetry points of (In,Ga)N with the rapid disintegration of the valence band Bloch character and the appearance of a pinned impurity band in Ga(N,P).

This work was funded by the U. S. Department of Energy, Office of Science, Basic Energy Science, Materials Science and Energy Division, under Contract No. DE-AC36-08GO28308 to NREL.

*alex.zunger@nrel.gov

[1] *Alloy Physics: A Comprehensive Reference*, edited by W. Pfeiler (Wiley-VCH, Weinheim, 2007).
[2] A. Zunger and S. Mahajan, *Handbook on Semiconductors* (Elsevier, Amsterdam, 1994), 2nd ed., Vol. 3, p. 1399.
[3] A.-B. Chen and A. Sher, *Semiconductor Alloys: Physics and Materials Engineering* (Plenum Press, New York, 1995).
[4] J. C. Mikkelsen and J. B. Boyce, Phys. Rev. Lett. **49**, 1412 (1982).
[5] D. G. Thomas, J. J. Hopfield, and C. J. Frosch, Phys. Rev. Lett. **15**, 857 (1965).
[6] S. Lai and M. V. Klein, Phys. Rev. Lett. **44**, 1087 (1980).
[7] S. Permogorov *et al.*, J. Lumin. **24–25**, 409 (1981).
[8] Z. W. Lu, S.-H. Wei, and A. Zunger, Phys. Rev. B **45**, 10 314 (1992).
[9] L.-W. Wang *et al.*, Phys. Rev. Lett. **80**, 4725 (1998).
[10] L. Bellaiche *et al.*, Appl. Phys. Lett. **74**, 1842 (1999).
[11] N. Y. Moghadam and G. M. Stocks, Phys. Rev. B **71**, 134421 (2005).
[12] W. Shan *et al.*, Phys. Rev. Lett. **82**, 1221 (1999).
[13] J. S. Faulkner and G. M. Stocks, Phys. Rev. B **21**, 3222 (1980).
[14] F. Masia *et al.*, Phys. Rev. B **73**, 073201 (2006).
[15] A. G. Thompson *et al.*, Phys. Rev. **146**, 601 (1966).
[16] J. Endicott *et al.*, Phys. Rev. B **72**, 041306(R) (2005).
[17] J. Hwang *et al.*, Appl. Phys. Lett. **52**, 308 (1988).
[18] T. G. Dargam, R. B. Capaz, and B. Koiller, Phys. Rev. B **56**, 9625 (1997).
[19] T. B. Boykin *et al.*, J. Phys. Condens. Matter **19**, 036203 (2007).
[20] S.-H. Wei and A. Zunger, Appl. Phys. Lett. **72**, 2011 (1998).
[21] Empirical pseudopotentials taken from L. Bellaiche *et al.*, Appl. Phys. Lett. **74**, 1842 (1999), refitted for corrected InN band gap of 0.76 eV.
[22] P. R. C. Kent and A. Zunger, Phys. Rev. B **64**, 115208 (2001).
[23] S. V. Dudiy, P. R. C. Kent, and A. Zunger, Phys. Rev. B **70**, 161304(R) (2004).
[24] T. Mattila and A. Zunger, Phys. Rev. B **58**, 1367 (1998).
[25] B. I. Shklovskii and A. L. Efros, *Electronic Properties of Doped Semiconductors*, Springer Series in Solid-State Sciences Vol. 45 (Springer Verlag, Berlin, 1984).
[26] B. Fluegel *et al.*, Phys. Rev. B **72**, 073203 (2005).
[27] Ref. [26] incorrectly contrasted their observation of *pinned* cluster states at $x_N < 0.1\%$ with previous predictions [22] of *shifting states above* the amalgamation point, $x_N > 0.1\%$. In fact, for $x_N < 0.1\%$, both experiment and theory show pinning, as noted in Dudiy *et al.*, Phys. Rev. B **74**, 155303 (2006).